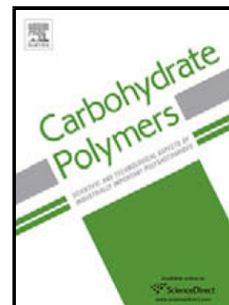


## Accepted Manuscript

Title: Fabrication of aggregation induced emission active Luminescent Chitosan Nanoparticles via a “one-pot” Multicomponent Reaction

Author: Qing Wan Meiyong Liu Dazhuang Xu Liucheng Mao Jianwen Tian Hongye Huang Peng Gao Fengjie Deng Xiaoyong Zhang Yen Wei



PII: S0144-8617(16)30815-3  
DOI: <http://dx.doi.org/doi:10.1016/j.carbpol.2016.07.026>  
Reference: CARP 11325

To appear in:

Received date: 8-4-2016  
Revised date: 5-7-2016  
Accepted date: 7-7-2016

Please cite this article as: Wan, Qing., Liu, Meiyong., Xu, Dazhuang., Mao, Liucheng., Tian, Jianwen., Huang, Hongye., Gao, Peng., Deng, Fengjie., Zhang, Xiaoyong., & Wei, Yen., Fabrication of aggregation induced emission active Luminescent Chitosan Nanoparticles via a “one-pot” Multicomponent Reaction. *Carbohydrate Polymers* <http://dx.doi.org/10.1016/j.carbpol.2016.07.026>

This is a PDF file of an unedited manuscript that has been accepted for publication. As a service to our customers we are providing this early version of the manuscript. The manuscript will undergo copyediting, typesetting, and review of the resulting proof before it is published in its final form. Please note that during the production process errors may be discovered which could affect the content, and all legal disclaimers that apply to the journal pertain.

Fabrication of aggregation induced emission active Luminescent Chitosan Nanoparticles via a “one-pot” Multicomponent Reaction

Qing Wan<sup>a,#</sup>, Meiyang Liu<sup>a,#</sup>, Dazhuang Xu<sup>a</sup>, Liucheng Mao<sup>a</sup>, Jianwen Tian<sup>a</sup>, Hongye Huang<sup>a</sup>, Peng Gao<sup>a</sup>, Fengjie Deng<sup>a,\*</sup>, Xiaoyong Zhang<sup>a,\*</sup>, Yen Wei<sup>b,\*</sup>

<sup>a</sup> Department of Chemistry and Jiangxi Provincial Key Laboratory of New Energy Chemistry, Nanchang University, 999 Xuefu Avenue, Nanchang 330031, China.

<sup>b</sup> Department of Chemistry and the Tsinghua Center for Frontier Polymer Research, Tsinghua University, Beijing, 100084, P. R. China.

# These authors contributed equally to this work

## Highlights

- Fabrication of aggregation induced emission active chitosan through a multicomponent reaction
- The multicomponent reaction can occur under rather mild experimental conditions
- The WS-Chitosan@An-CHO LPNs are promising for biological imaging applications
- The multicomponent reaction can also be utilized for fabrication of many other LPNs

## Abstract

Chitosan based nanomaterials have been extensively examined for biomedical applications for their biodegradability, low toxicity, biological activity and low cost. In this work, a novel strategy for fabrication of luminescent polymeric nanoparticles (LPNs) based on aggregation induced emission (AIE) dye and water soluble chitosan (WS-Chitosan) were firstly developed via a highly efficient mercaptoacetic acid (MA) locking imine reaction. In this multicomponent reaction (MCR), MA serves as “lock” to connect 9,10-Bis(aldehydephenyl)anthracene dye (An-CHO) and amino-containing WS-Chitosan under mild reaction conditions. The obtained WS-Chitosan@An-CHO LPNs show strong yellow emission and great water dispersibility. Biological evaluation results demonstrated that synthetic luminescent polymeric nanoparticles possess desirable cytocompatibility and distinct imaging properties. Therefore, we have developed a facile and useful method to fabricate AIE active nanoprobes with desirable properties for various biomedical applications. This strategy should be a general and

easy handling tool to fabricate many other AIE dye based materials.

**Keywords:** aggregation induced emission, water soluble chitosan, multicomponent reaction, luminescent polymeric nanoparticles, biomedical applications.

## 1. Introduction

In recent years, growing attentions have been paid to develop bioprobes based on luminescent polymeric nanoparticles (LPNs) for wide biomedical applications.(Liu et al., 2016; Liu et al., 2015; Nie, Xing, Kim & Simons, 2007; Wang, Yuan, Guo, Xu & Chen, 2014) Fluorescent imaging has been regarded as one of the useful tools to monitor the biological behavior process existed in complicated intracellular system with strong sensitivity and absolute inviolability,(Kang, Ha, Yun, Yu & Chang, 2011) and have been successfully applied as a versatile way for disease diagnosis,(Liu, Tu, Zhu, Ma & Chen, 2013) tracking and treatment.(Shi, Liu, Geng, Tang & Liu, 2012) So far, traditional luminescent probes were prepared based on some luminescent materials such as inorganic quantum dots(Wu et al., 2003; Zhang et al., 2013c) organic dyes,(Wang et al., 2005) organic dye-loaded silica nanoparticles and fluorescent proteins,(Heilemann et al., 2008) which were extensively applied in labeling cells and tissue specimens. Furthermore, the unique features such as high photostability and sensitivity of these luminescent materials make them allow real-time imaging of important intracellular molecules. Unfortunately, some vicious drawbacks existed in above-mentioned luminescent materials have become obstacle for their progress in cell labeling application. For example, inorganic quantum dots (Qdots) suffer from high toxicity when they were accumulated in cellular environment owing to the existence of heavy metal ions,(Derfus, Chan & Bhatia, 2004) which would cause terrible influence for human healthy. While dye-loaded silica nanoparticles possess poor biodegradability although they are highly luminescent and homogeneous.(Roy et al., 2005) The green fluorescent protein also encounter high cost, easy enzyme degradation, small Stokes shifts, terrible photostability and tedious transfection process and transfection efficiency,(Romantschuk et al., 2000) limiting their potential use in biomedical imaging application in spite of overcoming poor degradable problems bring from Qdots and fluorescent silica nanoparticles. Meanwhile, traditional organic dyes such as fluoresceins and rhodamines often suffer from luminescence quenching phenomena when presented in solution with high concentration or aggregated state, which was also called aggregation caused quenching (ACQ) effect. Therefore, in

order to conquer these problems of poor biodegradability, toxicity and ACQ effect, novel fluorescent materials with better optical and biological properties should be developed.

Aggregation induced emission (AIE) dyes were firstly reported by Tang *et al* in 2001.(Luo et al., 2001) AIE dyes emitted strong fluorescence in their aggregated state while non-fluorescence or weak fluorescence in dispersed state, which could effectively solve ACQ effect of conventional organic dyes. Since discovery, a number of AIE fluorogens such as siloles,(Wang, Zhang, Zhang, Zhu & Tang, 2010) cyano-substituted diarylethene,(Zhang et al., 2013a; Zhang, Ma, Liu, Zhang, Jia & Wei, 2013) tetraphenylethene,(Chi et al., 2012; Wan et al., 2016; Wan et al., 2015b; Wan et al., 2015c; Wu et al., 2012) triphenylethene,(Chen et al., 2012; Li et al., 2011; Zhang et al., 2011; Zhang et al., 2010; Zhang et al., 2014b) distyrylanthracene derivatives(Wang et al., 2013; Zhang et al., 2013f) have been synthesized and drastically investigated for their potential applications in fields such as bio/chem sensors, cell imaging and ion probes due to their excellent AIE characteristics, biodegradability and cytocompatibility. Up to now, some strategies for fabricating luminescent probes based on AIE dyes have drawn increasing attentions for their potential medical applications. Generally, two major methods for constructing LPNs based on AIE dyes have been developed, which contained non-covalent methods and covalent methods.(Huang et al., 2015; Liu et al., 2014a; Liu et al., 2014b; Zhang et al., 2014c; Zhang et al., 2013e) The non-covalent methods for preparing LPNs were that embedding the AIE dyes into the biocompatible amphiphilic polymers to obtain water dispersible luminescent nanoparticles. Other silica nanoparticles encapsulation and bovine serum albumin (BSA) implantation methods were also used to construct AIE active LPNs.(Qin et al., 2012; Zhang et al., 2013d; Zhang et al., 2014d) Nevertheless, the easy leakage of AIE dyes and separation of surface coating from LPNs have become serious restriction of non-covalent systems. On the other hand, covalent strategies to prepare LPNs could be summarized that reversible addition fragmentation chain transfer polymerization,(Zhang et al., 2014f) cross-linked Schiff based dynamic bonds,(Wan et al., 2015a; Yang et al., 2013; Zhang et al., 2013e) emulsion polymerization(Zhang et al., 2014e) and anhydride ring-opening reaction.(Zhang et al., 2014a) Based on these techniques, numerous AIE active LPNs with uniform size, great biocompatibility, high water dispersibility and strong luminescence have been fabricated and utilized for cell imaging. Although the impressive progress was made for fabrication of AIE active LPNs in methodology, more fabricated strategies with great stability, high-efficiency, short reaction time and environmentally friendly (catalyst free, room temperature condition and air atmosphere) and

multifunctional potential will receive more pursuit from scientists.

The water-soluble chitosan (named as WS-Chitosan) based luminescent nanoparticles have been intensively researched for biomedical applications due to their favorable features such as biocompatibility, non-toxicity and degradable potential.(Qi, Xu, Jiang, Hu & Zou, 2004) In this contribution, we report a robust synthesis protocol to prepare ultra-small cross-linked WS-Chitosan@An-CHO LPNs with uniform size, high water dispersibility, great biocompatibility and strong luminescent property via a “one-pot” multicomponent reaction (MCR).

## **2. Experimental**

### **2.1 Materials and methods**

All chemical agents were of analytical grade and used as received without any further purification. All the chemicals such as chitosan (deacetylation  $\geq 95\%$ , viscosity: 100-200 mpa.s), hydrogen peroxide (30 wt.%), ammonium persulphate (98%, 228.2 Da), anthracene (98%, 178.3 Da) and terephthalaldehyde (98%, 134.13 Da) were purchased from Aladdin Chemistry Co., Ltd (Shanghai, China). The dialysis bags (Size: 5 M, cut-off: 7000 Da) are purchased from Biotopped Co., Ltd (Beijing, China). All the other commercially available reagents were analytical grade and used without further purification.

$^1\text{H}$  NMR spectra were recorded on Bruker Avance-400 spectrometer with  $\text{D}_2\text{O}$  and  $\text{CDCl}_3$  as the solvents. The synthetic polymers and materials were characterized by Fourier transform infrared spectroscopy (FT-IR) using KBr pellets. The Fourier transform infrared (FT-IR) spectra were supplied from Nicolet5700 (Thermo Nicolet corporation). Transmission electron microscopy (TEM) images were recorded on a Hitachi 7650B microscope operated at 80 kV. The TEM specimens were got by putting a drop of the nanoparticle ethanol suspension on a carbon-coated copper grid. The size distribution of WS-Chitosan@An-CHO LNPs in phosphate buffered saline (PBS) was determined by dynamic laser scattering using a Zeta Plus particle size analyzer (Zeta Plus, Brookhaven Instruments, Holtsville, NY). The fluorescence data were obtained from the Fluorescence spectrophotometer (FSP, model: C11367-11), which purchased from Hamamatsu (Japanese).

### **2.2 Synthesis of 9, 10-Bis(bromomethyl)anthracene (Br-An-Br)**

The synthesis route of An-CHO was displayed in **Scheme S1**. At first, the intermediate products of 9, 10-Bis(bromomethyl)anthracene and 9,10-bis(diethylphosphorylmethyl)anthracene were synthesized by previous report.(Zhang et al., 2013d) For the preparation of 9,10-Bis(bromomethyl)anthracene: the

mixture of anthracene (7.6 g, 40 mmol), (CH<sub>2</sub>O)<sub>n</sub> (4.8 g), AlCl<sub>3</sub> (5.0 g) and solution of 33% HBr in acetic acid (60 mL) was stirring at 60 °C for 6 h. The obtained solid was put into water and stirring 30 min to remove residual reactants, filtration and dry in vacuum one night. The residue product was recrystallized in toluene three times to obtain yellow solid. Yield: 7.8 g (54%). <sup>1</sup>H NMR (300 MHz, CDCl<sub>3</sub>): δ 8.38 (m, 4H), δ 7.65 (m, 4H), δ 5.54 ppm (m, 4H).

### 2.3 Synthesis of 9,10-bis(diethylphosphorylmethyl)anthracene ((OEt)<sub>2</sub>(O)P-An-P(O)(OEt)<sub>2</sub>)

The 9, 10-Bis(bromomethyl)anthracene (1.2 g, 3.3 mmol) was mixed with triethyl phosphate (10 mL). Resulting mixture was refluxed at 180 °C for 8 h in order to obtain the pure product. The solvent was then removed at vacuum and the residue product was purified by a column chromatography on silica gel using ethyl acetate/CH<sub>2</sub>Cl<sub>2</sub> as the eluent. Yield: 1.05g (68%). <sup>1</sup>H NMR (300 MHz, CDCl<sub>3</sub>): δ 8.38 (m, 4H), δ 7.6 (m, 4H), 4.25 (d, 4H), 3.8 (m, 8H), 1.06 ppm (t, 12H).

### 2.4 synthesis of 9,10-Bis(aldehydephenyl)anthracene (CHO-An-CHO)

The 9, 10-Bis(aldehydephenyl)anthracene with unique AIE feature was synthesized by follows: synthetic 9,10-Bis(diethylphosphorylmethyl)anthracene (1.37 g, 3 mmol), terephthalaldehyde (1 g, 7.5 mmol) and t-BuOK (896 mg, 8 mmol) were mixed and stirring in dry tetrahydrofuran (THF) solution for 6 h at room temperature. The THF solution was removed by rotary evaporation and the residual solid was wash with water and extract with ethyl acetate for three times. The obtained organic layer was dried with anhydrous magnesium sulfate and purified by by a column chromatography on silica gel using ethyl acetate/petroleum ether (1/10) as the eluent. The result solid was faint yellow. Yield: 0.8 g (60.8%). <sup>1</sup>H NMR (300 MHz, CDCl<sub>3</sub>): δ 10.09 (d, 2H), δ 8.39 (m, 4H), δ 8.09 (m, 8H), δ 7.57 (m, 4H), 7.00 ppm (m, 4H).

### 2.5 preparation of water soluble chitosan (WS-Chitosan)

According to the previous report,(Tian, Liu, Hu & Zhao, 2004) the WS-Chitosan was prepared via depolymerisation of insoluble chitosan using H<sub>2</sub>O<sub>2</sub> as oxidant (**Scheme S2**). The purchased chitosan (4.8 g) was dissolved in the hydrochloric acid solution (100 mL, 0.5%) and then 12 mL H<sub>2</sub>O<sub>2</sub> (2.0 M) was added. The mixed solution was stirring at 50 °C for 4 h. After reaction, the mixed solution was filtrated. The filtrate was adjusted to pH = 7.0 using NaOH solution and WS-Chitosan could be obtained after adding excess ethanol. Thus obtained WS-Chitosan was dried in vacuum.

### 2.6 Preparation of cross-linked WS-Chitosan@An-CHO LPNs

The WS-Chitosan and An-CHO with strong yellow fluorescence were locked by mercaptoacetic acid

(MA) via a one-pot MCR reaction. Thus-obtained amphiphilic luminescent materials would self-assemble into nanoparticles and have promising application prospects for cell imaging. On the other hand, the synthetic route for preparation of WS-Chitosan@An-CHO LPNs via a one-pot MCR was shown in **Scheme 1**. WS-Chitosan (500 mg) in 2 mL distilled water was blended with An-CHO (75.4 mg, 0.17 mmol) in 5 mL THF and charged into a dry Schlenk tube. After then, Schlenk tube was placed in an oil bath at 30 °C for 30 min. Then, MA (156.4 mg, 1.7 mmol) was dropped gradually into the Schlenk tube and stirring for other 4 h. Finally, the resulting reactive raw products were purified by dialysis to remove residual reaction agents. The resultant products WS-Chitosan@An-CHO LPNs were dried at vacuum for further characterization.

## 2.7 Cytotoxicity evaluation of WS-Chitosan@An-CHO LPNs

In order to evaluate the harmful of WS-Chitosan@An-CHO LPNs for living cells, the cell viability of WS-Chitosan@An-CHO LPNs with strong yellow fluorescence on HeLa cells was evaluated by cell counting kit-8 (CCK-8) assay.(Zhang, Hu, Li, Tao & Wei, 2012; Zhang et al., 2015; Zhang et al., 2013b) The experimental procedure could be demonstrated by follows. Cells were put into 96-well microplates at a density of  $5 \times 10^4$  cells  $\text{mL}^{-1}$  in 160  $\mu\text{L}$  of respective medium containing 10% fetal bovine serum (FBS). After 24 h of cell attachment, WS-Chitosan@An-CHO LPNs with different final concentrations (10-100  $\mu\text{g mL}^{-1}$ ) were added and incubated with cells for 12 and 24 h. Then cells were repeatedly washed with PBS three times to remove noninternalized nanoparticles. 10  $\mu\text{L}$  of CCK-8 dye and 100  $\mu\text{L}$  of Dulbecco's modified eagle medium (DMEM) were added to each well and incubated for another 2 h. Afterward, plates were analyzed using a microplate reader (Victor III, Perkin-Elmer). Measurements of formazan dye absorbance were carried out at 450 nm, with the reference wavelength at 620 nm. The values were proportional to the number of live cells. The percent reduction of CCK-8 dye was compared to controls (cells without incubation with LPNs), which represented 100% CCK-8 reduction. Three replicate wells were used per microplate, and the experiment was operated for three times. Cell survival was expressed as absorbance relative to that of untreated controls. Results are presented as mean  $\pm$  standard deviation (SD).

## 2.8 Confocal microscopic imaging

HeLa cells were cultured in DMEM, supplemented with 10% heat-inactivated FBS, 2 mM glutamine, 100 U  $\text{mL}^{-1}$  penicillin, and 100  $\mu\text{g mL}^{-1}$  of streptomycin. Cell culture was controlled at 37 °C in a

similar humidified condition of 95% air and 5% CO<sub>2</sub> in culture medium. Culture medium should be updated every three days for maintaining the exponential growth of the cells. Before treatment, cells were seeded in a glass bottom dish with a density of 1×10<sup>5</sup> cells per dish. On the day of treatment, the cells were incubated with WS-Chitosan@An-CHO LPNs at a final concentration of 20 μg mL<sup>-1</sup> for 3 h at 37 °C. Afterward, the cells were washed three times with PBS to remove the Chitosan@An-CHO LPNs and then fixed with 4% paraformaldehyde for 10 min at room temperature. Cell images were obtained using a confocal laser scanning microscope (CLSM) Zesis 710 3-channel (Zesis, Germany) with the excitation wavelength of 458 nm.

### 3. Results and discussion

Fabrication of ultra-small AIE active LPNs with biodegradability and great biocompatibility is extremely important for intra-cellular bioimaging applications. As is well known, LPNs have been applied as effective and multifunctional nanoparticles capable of enhancing the diagnostic and therapeutic efficacy of imaging probes and targeted agents in cancer treatment due to the accumulation at solid tumor site of polymeric nanoparticles by the enhanced permeation and retention effect. In this work, we provide a robust method for the produce ultra-small cross-linked WS-Chitosan@An-CHO LPNs with well-dispersed in water via one-pot process under mild reaction conditions. The AIE fluorogen An-CHO was synthesized following prepared route described in afore-mentioned information. The successful synthesis of AIE dye could be confirmed by the <sup>1</sup>H NMR (**Fig. S1**). For fabrication of cross-linked WS-Chitosan@An-CHO LPNs, the hydrophobic AIE dyes (An-CHO) were conjugated with a hydrophilic and biodegradable biopolymer WS-Chitosan to form amphiphilic fluorescent materials via a one-pot MCR using MA as the lock. Thus obtained amphiphilic WS-Chitosan@An-CHO copolymers would self-assemble into nanoparticles of great stability in aqueous solution because of their cross-linked structure and excellent water dispersibility.

The successful synthesis of An-CHO and WS-Chitosan@An-CHO LPNs could be confirmed from the <sup>1</sup>H NMR spectra using CDCl<sub>3</sub> and D<sub>2</sub>O as solvents (**Fig. S1** and **Fig. 1**). As shown in **Fig. S1(b)**, the new peaks of chemical shift at 3.7-4.3 ppm represent the hydrogen atom of -CH<sub>2</sub> and -CH<sub>3</sub>. Compared with the <sup>1</sup>H NMR spectra of Br-An-Br, the appearance of new peak demonstrated that successful synthesis of (OEt)<sub>2</sub>(O)P-An-P(O)(OEt)<sub>2</sub>. The <sup>1</sup>H NMR spectrum of An-CHO was displayed in **Fig. S1(c)**. It suggested successful preparation of An-CHO dyes due to the appearance of new peak at 10.09

ppm, which is belonged to the aldehyde group. The chemical shift of each synthetic intermediate was described in the synthetic route. On the other hand, in order to prove successful formation of WS-Chitosan@An-CHO LPNs via conjugation of WS-Chitosan with An-CHO, two  $^1\text{H}$  NMR spectra of WS-Chitosan and WS-Chitosan@An-CHO LPNs are compared. As seen in **Fig. 1**, the multiplet peaks between 2.91 and 3.18 ppm for the WS-Chitosan@An-CHO sample are contributed to the  $-\text{CH}_2$  in the cross-linked heterocycle, which provide powerful evidence for successful formation of cross-linked structure. The peak of hydrogen atom of  $-\text{NH}_2$  existed in WS-Chitosan located at 5.01 ppm. However, peak intensity at the 5.01 ppm in WS-Chitosan@An-CHO was decreased as compared with WS-Chitosan (**Fig. 1**). This comparison indicated that partial amino groups have reacted with An-CHO. More importantly, some new peaks were found between 7.68 and 8.42 ppm, which could be ascribed to the peaks of aromatic rings of An-CHO. The above results demonstrated that successful fabrication of WS-Chitosan@An-CHO LPNs through a one-pot MCR.

Other than  $^1\text{H}$  NMR spectra, FT-IR spectra could also serve as powerful tool to confirm the cross-linked reaction between WS-Chitosan and An-CHO. As shown in **Fig. 2**, the FT-IR spectra are used to infer the functional groups in WS-Chitosan and WS-Chitosan@An-CHO LPNs. In general, the O-H stretching vibration is overlapped to the N-H stretching. The IR peak of amino and hydroxyl groups were appeared at ranging from 3200 to 3500  $\text{cm}^{-1}$ . (Wang, Wang, Jia, Li, Yu & Ding, 2014) After conjugating with An-CHO to prepare the WS-Chitosan@An-CHO LPNs, the absorption peak of amino groups is still existed. This could explain that amino groups of WS-Chitosan were partially reacted with An-CHO using MA as cross-linked reagent. Furthermore, the new peaks at 1650 and 1290  $\text{cm}^{-1}$  were assigned to the C-C(O)-N of heterocycle and C=C groups, respectively. These peaks are not found in the IR spectrum of WS-Chitosan, indicating that An-CHO has conjugated with chitosan successfully via MCR. Therefore, we could draw a conclusion that the fabricated method described in this work is capable for the preparation of AIE active LPNs through a facile one-pot MCR.

As well known, self-assembly of amphiphilic polymers to form nanoparticles is a facile and promising strategy for various biomedical applications. Therefore, the size and morphology of WS-Chitosan@An-CHO copolymers were characterized by TEM. As shown in **Fig. 3**, many uniform spherical nanoparticles with diameter ranging from 30-100 nm could be clearly observed, providing us

direct evidence that successfully self-assemble into nanoparticles of amphiphilic WS-Chitosan@An-CHO copolymers in aqueous solution. The size distribution of WS-Chitosan@An-CHO LNPs in PBS was determined using a ZetaPlus particle size analyzer. Due to their amphiphilic property, WS-Chitosan@An-CHO copolymers were self-assembled into nanoparticles in PBS. We found that hydrodynamic size distribution of WS-Chitosan@An-CHO LNPs was  $128.0 \pm 14.4$  nm (**Fig. S2**). The size distribution from DLS measurement is greater than the size from TEM characterization. This reason could be considered as the shrinkage of amphiphilic fluorescent polysaccharide under drying procedure. Therefore, according to the results of TEM image and DLS, we confirmed that successful preparation of AIE active luminescent nanoparticles based on the combination of WS-Chitosan and An-CHO by a MCR method. During the self-assembly procedure, the hydrophobic AIE dye An-CHO is expected to aggregate in the core of nanoparticles, which will result in enhanced luminescence emission due to the AIE feature of An-CHO. Herein, the UV absorption spectrum and fluorescent spectra are used to evaluate their water dispersibility and fluorescent property. From **Fig. 4A**, the strong absorption peak appears at 210 nm can be ascribed to K absorption band, suggesting that contained conjugated system of two double bonds ( $-C=C-C=C-$ ) in WS-Chitosan@An-CHO LPNs. Moreover, two strong absorption peaks at 273 and 281 nm were also detected by UV-Vis spectrum of WS-Chitosan@An-CHO LPNs. These peaks can be attributed to  $-C=C-$  substituent groups on aromatic rings. The adsorption peak at 432 nm is possibly ascribed to the redshift of  $n-\pi^*$  transition, which implied that hetero atoms such as O, N or S were linked with the aromatic rings. Furthermore, WS-Chitosan@An-CHO copolymers showed great dispersibility in water. For example, the background of “AIE” word could be clearly observed in inset of **Fig. 4A**. These results clearly confirm the successful conjugation of WS-Chitosan with An-CHO via a simple one-pot MCR. The fluorescent spectra of WS-Chitosan@An-CHO LPNs were shown in **Fig. 4B**. The maximum emission wavelength of WS-Chitosan@An-CHO LPNs was centered at 558 nm, while the optimal fluorescent excitation wavelength was located at 436 nm. Meanwhile, the strong yellow luminescence could be observed under irradiating by UV lamp at 365 nm (inset of **Fig. 4B**). This suggested that the AIE feature of WS-Chitosan@An-CHO LPNs could efficiently overcome the ACQ effect of LPNs based on conventional organic dyes.

The fluorescent properties such as intensity and photostability of LPNs play an important role in

their biomedical applications. **Fig. S3** shows the photoluminescence (PL) spectra of WS-Chitosan@An-CHO LPNs before and after continuously irradiating with UV lamp at 365 nm for 2 h. As compared with the PL intensity before irradiating, the fluorescent intensity was decreased in some extent (**Fig. S3**). The above comparison suggested that the WS-Chitosan@An-CHO LPNs excellent photostability, making them for more suitable for biological imaging especially for long time tracing. In order to evaluate the potential biomedical application of WS-Chitosan@An-CHO LPNs, the cell viability of WS-Chitosan@An-CHO LPNs towards HeLa cells was determined CCK-8 assay. Cells were incubated with different concentrations of WS-Chitosan@An-CHO LPNs for 12 and 24 h. As shown in **Fig. 5**, the cell viability values have not obviously changed under the experimental conditions. The cell viability values are still greater than 95% even the particle concentration is greater than 100  $\mu\text{g mL}^{-1}$  for 24 h incubation. The half maximal inhibitory concentration ( $\text{IC}_{50}$ ) values of WS-Chitosan@An-CHO LPNs at 12 and 24 h incubation were calculated to be 1630.3 and 422.3  $\mu\text{g mL}^{-1}$ , respectively. The cell viability results indicated that WS-Chitosan@An-CHO LPNs possess good biocompatibility. On the other hand, WS-Chitosan has been extensively examined for various biomedical applications such as drug and gene delivery, antibacterial, tissue engineering and cell encapsulation for its good biocompatibility, degradable and low cost and some specific biological activity. Therefore, the WS-Chitosan@An-CHO LPNs should also be used for fabrication of multifunctional biomaterials for various biomedical applications.

Considered the properties such as good water dispersibility, strong yellow fluorescence, uniform morphology and facile fabrication procedure, the possible biomedical applications of WS-Chitosan@An-CHO LPNs were evaluated based on their cell uptake behavior. Their cell uptake behavior was evaluated by CLSM observation (**Fig. 6**). **Fig. 6A** shows the fluorescent image of HeLa cells, which were incubated with 20  $\mu\text{g mL}^{-1}$  WS-Chitosan@An-CHO LPNs for 3 h. It can be seen that strong fluorescent signals spread over cells could be clearly observed. However, in the centre of cells, relative weak fluorescent signals are found. These areas should be ascribed to the location of cell nucleus. The above results implied that cell uptakes of WS-Chitosan@An-CHO LPNs may be mainly caused by typical endocytosis route. In addition, we can find that cells still adhered to cell plates very well and kept their normal morphology (**Fig. 6B**). This also confirmed the good biocompatibility of WS-Chitosan@An-CHO LPNs. **Fig. 6C** showed the emerged image of **Fig. 6A** and **Fig. 6B**. It can be

clearly observed that the fluorescent areas are overlapped with the location of cells, and the cell nucleus is surrounded by the fluorescent signals, implied that WS-Chitosan@An-CHO LPNs are mainly distributed in the cytoplasm after endocytosis. As compared with the IC50 values of WS-Chitosan@An-CHO LPNs, the dosage used for cell imaging applications is much less. Therefore, considered the good biocompatibility, efficient cell uptake and imaging performance of WS-Chitosan@An-CHO LPNs, we could conclude that WS-Chitosan@An-CHO LPNs are promising candidates for biological imaging applications.

#### **4. Conclusion**

In summary, luminescent chitosan nanoparticles with AIE feature were hastily prepared for the first time through a one-pot MCR, which relied on the MA as the lock to form covalent linkage between the amino groups of WS-Chitosan and aldehyde groups of AIE dye. The obtained amphiphilic WS-Chitosan@An-CHO copolymers could self-assemble into ultrabright LPNs in aqueous solution because of hydrophobic AIE dyes as core while hydrophilic chitosan as shell, the biocompatibility and cell uptake behavior of WS-Chitosan@An-CHO LPNs suggested their potential application prospect in biomedical fields. In addition, the MCR can occur under rather mild experimental conditions such as catalyst-free, efficient, atom-economical and multifunctional potential. On the other hand, many other AIE active nanoparticles with different functional components and properties can also be fabricated based on the similar MCR reaction where the properties of AIE dyes and polymers can be adjusted and designed according to our demand. Furthermore, numerous functional groups were existed in WS-Chitosan@An-CHO LPNs, which could be utilized for conjugation with other functional components such as drugs, target agents and other imaging probes. Last but not least, many other components such as antibodies and functional polymers could also be introduced into these AIE active polymeric systems through adding them into the reaction system in one-pot. Therefore, we could conclude that WS-Chitosan@An-CHO LPNs to be promising biomaterials for various biomedical applications.

#### **Acknowledgements**

This research was supported by the National Science Foundation of China (Nos. 51363016, 21474057, 21564006, 21561022), and the National 973 Project (Nos. 2011CB935700).

## References

- Chen, C., Liao, J. Y., Chi, Z., Xu, B., Zhang, X., Kuang, D. B., Zhang, Y., Liu, S., & Xu, J. (2012). Metal-free organic dyes derived from triphenylethylene for dye-sensitized solar cells: tuning of the performance by phenothiazine and carbazole. *J. MATER. CHEM.*, *22*(18), 8994-9005.
- Chi, Z., Zhang, X., Xu, B., Zhou, X., Ma, C., Zhang, Y., Liu, S., & Xu, J. (2012). Recent advances in organic mechanofluorochromic materials. *CHEM. SOC. REV.*, *41*(10), 3878-3896.
- Derfus, A. M., Chan, W. C., & Bhatia, S. N. (2004). Probing the cytotoxicity of semiconductor quantum dots. *NANO LETT.*, *4*(1), 11-18.
- Heilemann, M., van de Linde, S., Schüttelz, M., Kasper, R., Seefeldt, B., Mukherjee, A., Tinnefeld, P., & Sauer, M. (2008). Subdiffraction - resolution fluorescence imaging with conventional fluorescent probes. *Angew. Chem. Int. Edit.*, *47*(33), 6172-6176.
- Huang, Z., Zhang, X., Zhang, X., Fu, C., Wang, K., Yuan, J., Tao, L., & Wei, Y. (2015). Amphiphilic fluorescent copolymers via one-pot combination of chemoenzymatic transesterification and RAFT polymerization: synthesis, self-assembly and cell imaging. *Polym. Chem.*, *6*(4), 607-612.
- Kang, N. Y., Ha, H. H., Yun, S. W., Yu, Y. H., & Chang, Y. T. (2011). Diversity-driven chemical probe development for biomolecules: beyond hypothesis-driven approach. *CHEM. SOC. REV.*, *40*(7), 3613-3626.
- Li, X. F., Chi, Z. G., Xu, B. J., Li, H. Y., Zhang, X. Q., Zhou, W., Zhang, Y., Liu, S. W., & Xu, J. R. (2011). Synthesis and characterization of triphenylethylene derivatives with aggregation-induced emission characteristics. *J. Fluoresc.*, *21*(5), 1969-1977.
- Liu, M., Huang, H., Wang, K., Xu, D., Wan, Q., Tian, J., Huang, Q., Deng, F., Zhang, X., & Wei, Y. (2016). Fabrication and Biological Imaging Application of AIE-active Luminescent Starch based Nanoprobes. *Carbohydr. Polym.*, *142*, 38-44.
- Liu, M., Zhang, X., Yang, B., Deng, F., Huang, Z., Yang, Y., Li, Z., Zhang, X., & Wei, Y. (2014a). Ultrabright and biocompatible AIE dye based zwitterionic polymeric nanoparticles for biological imaging. *RSC ADV.*, *4*(66), 35137-35143.
- Liu, M., Zhang, X., Yang, B., Li, Z., Deng, F., Yang, Y., Zhang, X., & Wei, Y. (2015). Fluorescent nanoparticles from starch: Facile preparation, tunable luminescence and bioimaging. *Carbohydr. Polym.*, *121*, 49-55.
- Liu, M., Zhang, X., Yang, B., Liu, L., Deng, F., Zhang, X., & Wei, Y. (2014b). Polylysine Crosslinked AIE Dye Based Fluorescent Organic Nanoparticles for Biological Imaging Applications. *Macromol. Biosci.*, *14*(9), 1260-1267.
- Liu, Y., Tu, D., Zhu, H., Ma, E., & Chen, X. (2013). Lanthanide-doped luminescent nano-bioprobes: from fundamentals to biodetection. *Nanoscale*, *5*(4), 1369-1384.
- Luo, J., Xie, Z., Lam, J. W., Cheng, L., Chen, H., Qiu, C., Kwok, H. S., Zhan, X., Liu, Y., & Zhu, D. (2001). Aggregation-induced emission of 1-methyl-1, 2, 3, 4, 5-pentaphenylsilole. *CHEM. COMMUN.*(18), 1740-1741.
- Nie, S., Xing, Y., Kim, G. J., & Simons, J. W. (2007). Nanotechnology applications in cancer. *Annu. Rev. Biomed. Eng.*, *9*, 257-288.
- Qi, L., Xu, Z., Jiang, X., Hu, C., & Zou, X. (2004). Preparation and antibacterial activity of chitosan nanoparticles. *Carbohydr. Res.*, *339*(16), 2693-2700.
- Qin, W., Ding, D., Liu, J., Yuan, W. Z., Hu, Y., Liu, B., & Tang, B. Z. (2012). Biocompatible Nanoparticles with Aggregation-Induced Emission Characteristics as Far-Red/Near-Infrared Fluorescent Bioprobes for In Vitro and In Vivo Imaging Applications. *Adv. Funct. Mater.*, *22*(4), 771-779.

Romantschuk, M., Sarand, I., Petänen, T., Peltola, R., Jonsson Vihanne, M., Koivula, T., Yrjälä, K., & Haahtela, K. (2000). Means to improve the effect of in situ bioremediation of contaminated soil: an overview of novel approaches. *Environ. Pollut.*, *107*(2), 179-185.

Roy, I., Ohulchanskyy, T. Y., Bharali, D. J., Pudavar, H. E., Mistretta, R. A., Kaur, N., & Prasad, P. N. (2005). Optical tracking of organically modified silica nanoparticles as DNA carriers: a nonviral, nanomedicine approach for gene delivery. *P. Natl. Acad. Sci. USA.*, *102*(2), 279-284.

Shi, H., Liu, J., Geng, J., Tang, B. Z., & Liu, B. (2012). Specific Detection of Integrin  $\alpha\beta 3$  by Light-Up Bioprobe with Aggregation-Induced Emission Characteristics. *J. Am. Chem. Soc.*, *134*(23), 9569-9572.

Tian, F., Liu, Y., Hu, K., & Zhao, B. (2004). Study of the depolymerization behavior of chitosan by hydrogen peroxide. *Carbohydr. Polym.*, *57*(1), 31-37.

Wan, Q., He, C., Wang, K., Liu, M., Huang, H., Huang, Q., Deng, F., Zhang, X., & Wei, Y. (2015a). Preparation of Ultrabright AIE Nanoprobes via Dynamic Bonds. *Tetrahedron*, *71*(46), 8791-8797.

Wan, Q., Liu, M., Xu, D., Huang, H., Mao, L., Zeng, G., Deng, F., Zhang, X., & Wei, Y. (2016). Facile fabrication of amphiphilic AIE active glucan via formation of dynamic bonds: self assembly, stimuli responsiveness and biological imaging. *J. Mater. Chem. B*, *4*(22), 4033-4039.

Wan, Q., Wang, K., Du, H., Huang, H., Liu, M., Deng, F., Dai, Y., Zhang, X., & Wei, Y. (2015b). A rather facile strategy for the fabrication of PEGylated AIE nanoprobes. *Polym. Chem.*, *6*(29), 5288-5294.

Wan, Q., Wang, K., He, C., Liu, M., Zeng, G., Huang, H., Deng, F., Zhang, X., & Wei, Y. (2015c). Stimulus Responsive Cross-linked AIE-active polymeric Nanoprobes: Fabrication and Biological Imaging Application. *Polym. Chem.*, *6*(47), 8214-8221.

Wang, K., Yuan, X., Guo, Z., Xu, J., & Chen, Y. (2014). Red emissive cross-linked chitosan and their nanoparticles for imaging the nucleoli of living cells. *Carbohydr. Polym.*, *102*, 699-707.

Wang, L., Yan, R., Huo, Z., Wang, L., Zeng, J., Bao, J., Wang, X., Peng, Q., & Li, Y. (2005). Fluorescence Resonant Energy Transfer Biosensor Based on Upconversion - Luminescent Nanoparticles. *Angewandte Chemie International Edition*, *44*(37), 6054-6057.

Wang, M., Zhang, G., Zhang, D., Zhu, D., & Tang, B. Z. (2010). Fluorescent bio/chemosensors based on silole and tetraphenylethene luminogens with aggregation-induced emission feature. *J. MATER. CHEM.*, *20*(10), 1858-1867.

Wang, N., Wang, X., Jia, Y., Li, X., Yu, J., & Ding, B. (2014). Electrospun nanofibrous chitosan membranes modified with polyethyleneimine for formaldehyde detection. *Carbohydr. Polym.*, *108*, 192-199.

Wang, Z., Xu, B., Zhang, L., Zhang, J., Ma, T., Zhang, J., Fu, X., & Tian, W. (2013). Folic Acid-functionalized Mesoporous Silica nanospheres Hybridized with AIE Luminogens for Targeted Cancer Cell Imaging. *Nanoscale*, *5*(5), 2065-2072.

Wu, W., Ye, S., Huang, L., Xiao, L., Fu, Y., Huang, Q., Yu, G., Liu, Y., Qin, J., & Li, Q. (2012). A conjugated hyperbranched polymer constructed from carbazole and tetraphenylethylene moieties: convenient synthesis through one-pot "A 2+ B 4" Suzuki polymerization, aggregation-induced enhanced emission, and application as explosive chemosensors and PLEDs. *J. MATER. CHEM.*, *22*(13), 6374-6382.

Wu, X., Liu, H., Liu, J., Haley, K. N., Treadway, J. A., Larson, J. P., Ge, N., Peale, F., & Bruchez, M. P. (2003). Immunofluorescent labeling of cancer marker Her2 and other cellular targets with semiconductor quantum dots. *Nat. Biotechnol.*, *21*(1), 41-46.

Yang, M., Xu, D., Xi, W., Wang, L., Zheng, J., Huang, J., Zhang, J., Zhou, H., Wu, J., & Tian, Y. (2013). Aggregation-induced fluorescence behavior of triphenylamine-based Schiff bases: the combined effect of multiple forces. *J. Org. Chem.*, *78*(20), 10344-10359.

Zhang, X., Chi, Z., Xu, B., Li, H., Yang, Z., Li, X., Liu, S., Zhang, Y., & Xu, J. (2011). Synthesis of blue light emitting bis (triphenylethylene) derivatives: a case of aggregation-induced emission enhancement. *Dyes Pigments*, *89*(1), 56-62.

Zhang, X., Hu, W., Li, J., Tao, L., & Wei, Y. (2012). A Comparative Study of Cellular Uptake and Cytotoxicity of Multi-walled Carbon Nanotube, Graphene Oxide, and Nanodiamond. *Toxicol. Res.*, *1*(1), 62-68.

Zhang, X., Liu, M., Yang, B., Zhang, X., Chi, Z., Liu, S., Xu, J., & Wei, Y. (2013a). Cross-linkable Aggregation Induced Emission Dye Based Red Fluorescent Organic Nanoparticles and Their Cell Imaging Applications. *Polym. Chem.*, *4*(19), 5060-5064.

Zhang, X., Liu, M., Zhang, X., Deng, F., Zhou, C., Hui, J., Liu, W., & Wei, Y. (2015). Interaction of Tannic Acid with Carbon Nanotubes: Enhancement of Dispersibility and Biocompatibility. *Toxicol. Res.*, *4*(1), 160-168.

Zhang, X., Ma, Z., Liu, M., Zhang, X., Jia, X., & Wei, Y. (2013). A new organic far-red mechanofluorochromic compound derived from cyano-substituted diarylethene. *Tetrahedron*, *69*(49), 10552-10557.

Zhang, X., Wang, S., Liu, M., Hui, J., Yang, B., Tao, L., & Wei, Y. (2013b). Surfactant-dispersed Nanodiamond: Biocompatibility Evaluation and Drug Delivery Applications. *Toxicol. Res.*, *2*(5), 335-346.

Zhang, X., Wang, S., Zhu, C., Liu, M., Ji, Y., Feng, L., Tao, L., & Wei, Y. (2013c). Carbon-dots Derived from Nanodiamond: Photoluminescence Tunable Nanoparticles for Cell Imaging. *J. Colloid Interf. Sci.*, *397*(9), 39-44.

Zhang, X., Yang, Z., Chi, Z., Chen, M., Xu, B., Wang, C., Liu, S., Zhang, Y., & Xu, J. (2010). A multi-sensing fluorescent compound derived from cyanoacrylic acid. *J. Mater. Chem.*, *20*(2), 292-298.

Zhang, X., Zhang, X., Wang, S., Liu, M., Zhang, Y., Tao, L., & Wei, Y. (2013d). Facile Incorporation of Aggregation-induced Emission Materials into Mesoporous Silica Nanoparticles for Intracellular Imaging and Cancer Therapy. *ACS Appl. Mater. Interf.*, *5*(6), 1943-1947.

Zhang, X., Zhang, X., Yang, B., Hui, J., Liu, M., Chi, Z., Liu, S., Xu, J., & Wei, Y. (2014a). Facile Preparation and Cell Imaging Applications of Fluorescent Organic Nanoparticles that Combine AIE Dye and Ring-opening Polymerization. *Polym. Chem.*, *5*(2), 318-322.

Zhang, X., Zhang, X., Yang, B., Hui, J., Liu, M., Chi, Z., Liu, S., Xu, J., & Wei, Y. (2014b). A Novel Method for Preparing AIE Dye based Cross-linked Fluorescent Polymeric Nanoparticles for Cell Imaging. *Polym. Chem.*, *5*(3), 683-688.

Zhang, X., Zhang, X., Yang, B., Hui, J., Liu, M., Liu, W., Chen, Y., & Wei, Y. (2014c). PEGylation and Cell Imaging Applications of AIE Based Fluorescent Organic Nanoparticles via Ring-opening Reaction. *Polym. Chem.*, *5*(3), 689-693.

Zhang, X., Zhang, X., Yang, B., Liu, L., Hui, J., Liu, M., Chen, Y., & Wei, Y. (2014d). Aggregation-induced Emission Dyes Based Luminescent Silica Nanoparticles: Facile Preparation, Biocompatibility Evaluation and Cell Imaging Applications. *RSC Adv.*, *4*(20), 10060-10066.

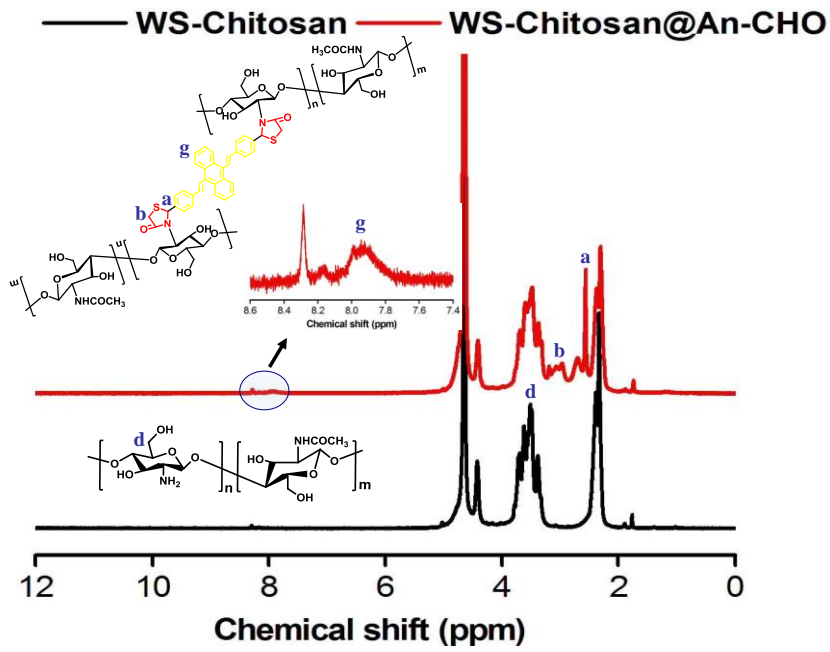
Zhang, X., Zhang, X., Yang, B., Liu, M., Liu, W., Chen, Y., & Wei, Y. (2013e). Facile fabrication and cell imaging applications of aggregation-induced emission dye-based fluorescent organic nanoparticles. *Polym. Chem.*, *4*(16), 4317-4321.

Zhang, X., Zhang, X., Yang, B., Liu, M., Liu, W., Chen, Y., & Wei, Y. (2014e). Fabrication of Aggregation Induced Emission Dye-based Fluorescent Organic Nanoparticles via Emulsion Polymerization and Their Cell Imaging Applications. *Polym. Chem.*, *5*(2), 399-404.

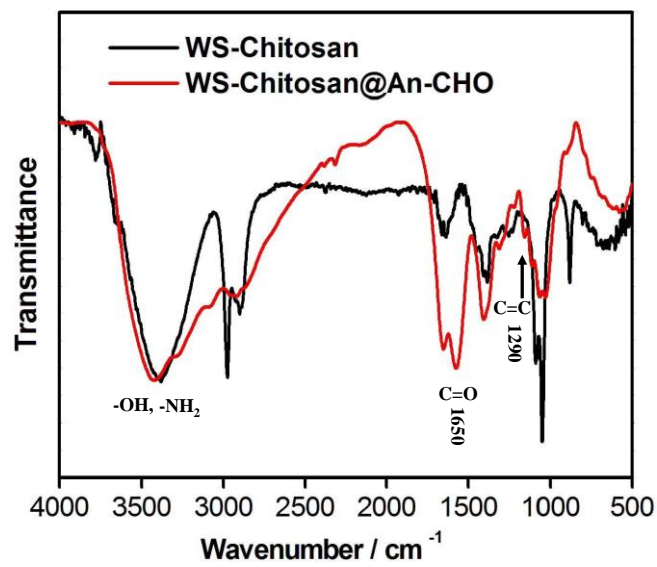
Zhang, X., Zhang, X., Yang, B., Liu, M., Liu, W., Chen, Y., & Wei, Y. (2014f). Polymerizable

aggregation-induced emission dye-based fluorescent nanoparticles for cell imaging applications. *Polym. Chem.*, 5(2), 356-360.

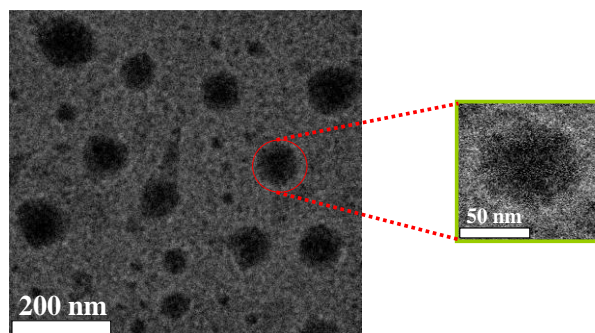
Zhang, X., Zhang, X., Yang, B., Wang, S., Liu, M., Zhang, Y., Tao, L., & Wei, Y. (2013f). Aggregation-induced emission material based fluorescent organic nanoparticles: facile PEGylation and cell imaging applications. *RSC ADV.*, 3(25), 9633-9636.



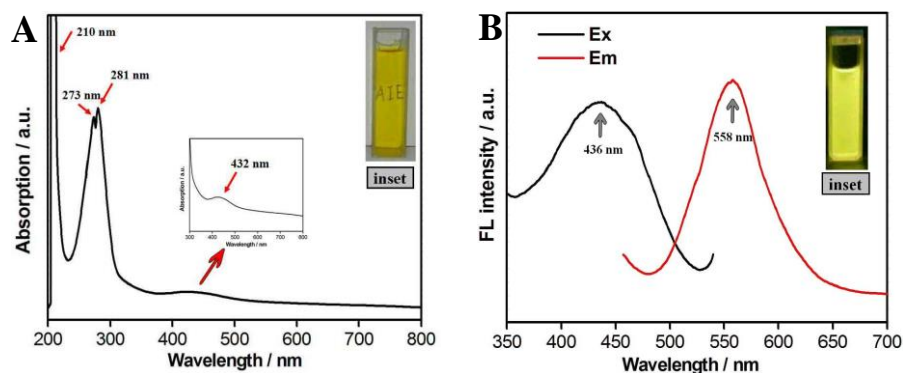
**Fig.1** The  $^1\text{H}$  NMR spectra of WS-Chitosan and WS-Chitosan@An-CHO LPNs.



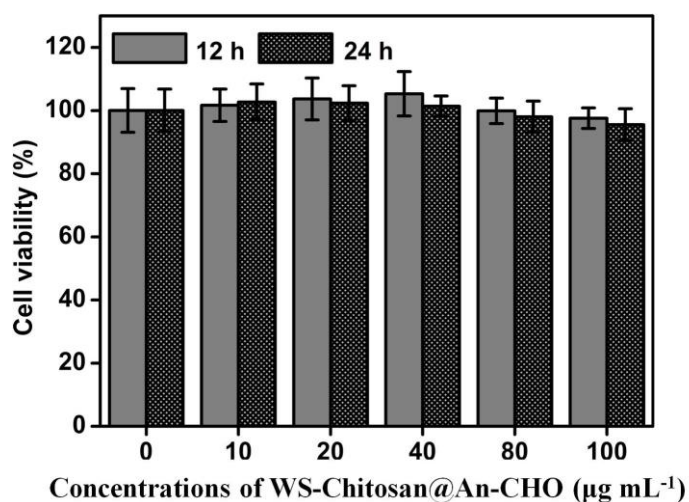
**Fig. 2** Representative FT-IR spectra of WS-Chitosan and WS-Chitosan@An-CHO LPNs.



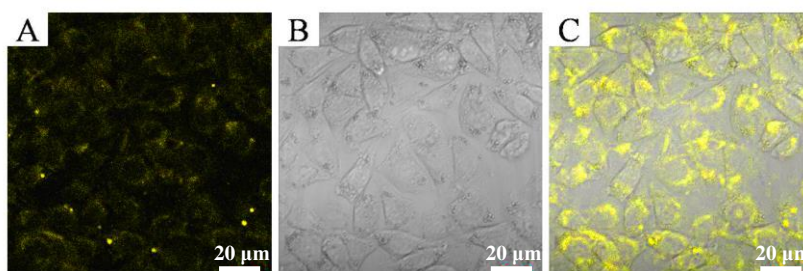
**Fig. 3** TEM images of WS-Chitosan@An-CHO LPNs.



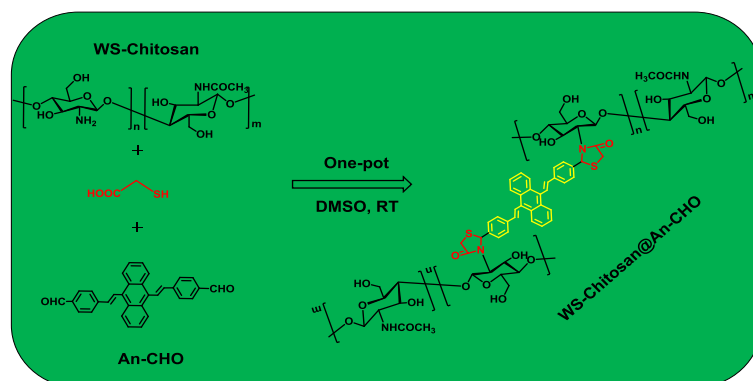
**Fig. 4** (A) The UV-Vis absorption spectrum of WS-Chitosan@An-CHO LPNs dispersed in water, the inset picture using “AIE” as background demonstrate that great water dispersibility of WS-Chitosan@An-CHO LPNs. (B) The excitation (Ex) and emission (Em) fluorescent spectra of WS-Chitosan@An-CHO LPNs. The inset picture suggests strong fluorescence emission of WS-Chitosan@An-CHO LPNs.



**Fig. 5** Cell viability evaluation of WS-Chitosan@An-CHO LPNs towards HeLa cells based on CCK-8 assay. The HeLa cells were incubated with 10-100 µg mL<sup>-1</sup> LPNs for 12 and 24 h.



**Fig. 6** CLSM images of HeLa cells incubated with 20 µg mL<sup>-1</sup> WS-Chitosan@An-CHO LPNs for 3 h. (A) excited with 405 nm, (B) bright field, (C) merged image of A and B. Scale bar = 20 µm.



**Scheme 1** The synthetic route of WS-Chitosan@An-CHO LPNs using WS-Chitosan, An-CHO and MA as the reaction agents.